CHEMCONFLUX[20] Special Issue

J. Indian Chem. Soc.,
Vol. 97, No. 10a, October 2020, pp. 1737-1745

Neuro-estimator based generic model control of a non-linear CSTR having multiplicity

Siddharth Gumber[a], Vinodh Kumar[b] and Dipesh S. Patle*[c]

[a]School of Mechanical Engineering, [b]School of Electrical Engineering,
Vellore Institute of Technology Vellore, Vellore-632 014, Tamil Nadu, India

[c]Chemical Engineering Department, Motilal Nehru National Institute of Technology, Allahabad,
Prayagraj-211 004, Uttar Pradesh, India

E-mail: dipesh-patle@mnnit.ac.in

Manuscript received online 24 July 2020, revised and accepted 23 August 2020

The control of a non-linear jacketed Continuous Stirred Tank Reactor (CSTR) with steady-state multiplicity is challenging due to its unstable nature. Generally, CSTR is operated near/at unstable equilibrium nodes, which decides the optimal productivity of the process. In this paper, a neural-estimator based non-linear control structure is developed for a CSTR possessing multiplicity. A Neuro-estimator based on feed-forward neural network has been designed to estimate the reactor concentration, which is often an imprecisely known parameter of the CSTR. We integrate the Neuro-estimator with a generic model controller (GMC) to develop a Neuro-GMC structure which utilizes the concentration estimated by the Neuro-estimator. Both servo and regulatory studies are performed to assess the effectiveness of the Neuro-GMC in controlling the reactor. Two additional control schemes, namely an extended Internal Model Control (IMC) and a standard PI controller, are designed to compare performance of the designed Neuro-GMC. Simulation results highlight that even in the presence of process-model mismatch, the Neuro-GMC yields better tracking and disturbance rejection characteristics.

Keywords: Advanced process control, Neuro-estimator, GMC, IMC, CSTR.

Introduction

Occurrence of steady-state multiplicity in CSTR poses difficulty in its control. Many researchers[1,2] studied the non-linear characteristics of a CSTR and have developed schemes to linearize the system. Globally linearizing control (GLC) involves imparting linear features into the non-linear process model. Extensive research has been conducted in evolving the GLC algorithm, but one requires exact knowledge of the system dynamics, which is often difficult to ascertain.

Mujtaba *et al.*[3] developed non-linear model based control techniques for batch reactors using neural networks. The study shows that a neural network based IMC requires a deep training and insight of the process to cope with performance uncertainties. Czeczot[4] developed a balance-based adaptive control for a non-isothermal CSTR. The author noticed control related difficulties during large fluctuations in the flow-rate. Hence, it is beneficial to integrate an estimator/observer when using model based controller to compensate for the process-model mismatch. A novel feedback predictive control algorithm was developed and evaluated by Rollins and Mei[5]. They used a time-delay in the manipulated variable (not in the controlled variable), which was addressed by approaches such as the Smith Predictor. Jana[6] developed adaptive state estimator based GMC and showed that this combined control scheme outperforms a conventional PI controller.

GMC relies on accurate information of the process dynamics. Process/model mismatch is a common problem whilst dealing with non-linear processes such as in a non-isothermal adiabatic CSTR which possesses multiplicity. Adaptive state estimators/observers (ASE/ASO) have been developed by many researchers[6] which require controlled and manipulated variables as inputs. A hybrid control mechanism combining GMC and a capable estimator can provide a better closed-loop performance as all the required states are not prudently measurable in many processes[7,8]. Other major advantages of the GMC controller are its simple design

and tuning. It also allows the non-linear governing equations to be incorporated directly into the algorithmic treatise[7].

It is evident that Neuro-GMC and extended-IMC are both model-based advanced controllers, but it is indeed crucial to present a comparison with respect to PI controller also. In what follows, we list important pointers pertaining to the use of PI controllers: (1) Despite being a conventional and non-model based controller, PI is one of the most commonly used controllers in Chemical industry, (2) earlier studies have reported that PI can provide satisfactory performance even for non-linear processes and (3) it is important to ascertain the extent of superiority of model-based controllers as opposed to a standard PI controller as advanced controllers require greater efforts and cost. Hence, only a fair comparison can guide a control engineer about the worth of additional efforts and cost incurred in the development of such controllers.

The main focus of this research is to establish an optimal control mechanism that can be employed to control a non-linear CSTR that has steady state multiplicity features. The main highlight of the present study is accurate estimation of the imprecisely known parameter, 'concentration' based on the only available variable i.e. temperature. In addition, an extended IMC and a conventional PI controller have been developed to compare the performance obtained from the Neuro-GMC feedback when applied to the CSTR. The performance is evaluated in terms of settling time, rise-time and total variation in manipulated variable (TV) defined as the summation of all control moves.

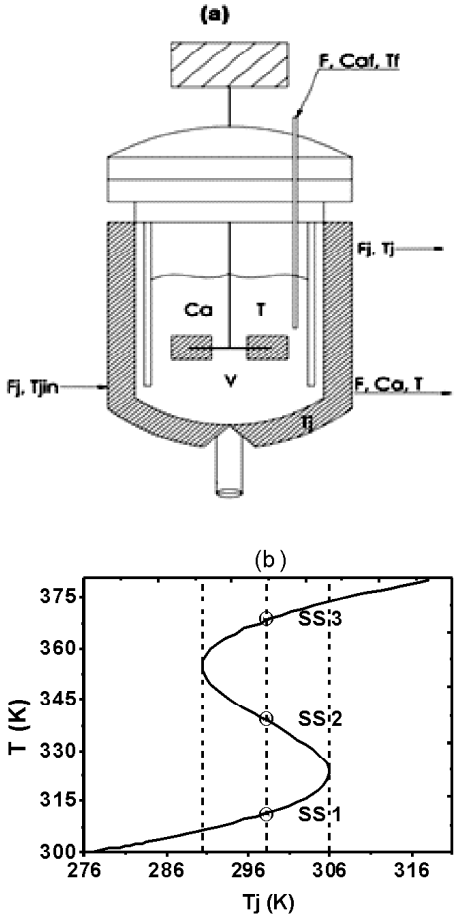

Fig. 1. (a) Schematic representation of a jacketed CSTR; (b) Multiplicity in CSTR-reactor temperature T vs jacket temperature T_j.

Process

Fig. 1a presents the example process considered in this study. A first order, exothermic, and an irreversible reaction takes place in a perfectly-mixed CSTR whose design parameters are presented in Table 1[6].

The non-isothermal adiabatic CSTR exhibits multiplicity and thus invokes the need for developing a control approach that affords a better reactor conversion whilst still operating the reactor at desired temperature. A CSTR generally exhibits three states namely: SS1, SS2 and SS3 as shown in Fig. 1b. It is clearly evident that operating the reactor at SS3 (in Fig. 1b) would produce high conversion but a high reactor temperature may destroy the catalyst and/or degrade the product. On the other hand, if the reactor is operated at SS1,

Table 1. Design parameters of the CSTR

Parameter	Value	Unit
C_A	8.5615	kmol/m^3
C_{Af}	10.0	kmol/m^3
F/V	1.0	hr^{-1}
ρC_p	500.0	kcal/m^3 °C
U_oA/V	150.0	kcal/m^3° C (hr)
T	38.2	°C
T_f	25.0	°C
T_j	25.0	°C
E	11843.0	kcal/kmol
$-\Delta H$	5960.0	kcal/kmol
Δt	0.005	hr
K_o	34930800.0	hr^{-1}
R	1.987	kcal/kmol K

a favourable reactor temperature will yield less conversion. Therefore, to optimise the conversion, one needs to operate at a non-linear, unstable SS2 state. This also defines the motivation for this study where GMC backed by a sophisticated F-ANN predictor yields a favourable conversion keeping the system stable at SS2.

The main-stay of a GMC control is its ability to consume the non-linear process model directly into the controller itself without having to linearise the model first. Table 2 presents multiple operating points of the reactor including highly non-linear SS2.

Table 2. Multiple steady state operating points (T_{ss} and C_{Ass} denote steady state temperature and concentration)

Steady state operating point	T_{ss} (K)	C_{Ass} (kmol/m^3)
SS1	311.2	8.5615
SS2	339.1	5.518
SS3	368.1	2.359

Eqs. (1) and (2) describe the mass and the energy balance for the CSTR:

$$\frac{dC_A}{dt} = \frac{F}{V}(C_{Af} - C_A) - K_o \exp\left(\frac{-\Delta E}{RT}\right) C_A \qquad (1)$$

$$\frac{dT}{dt} = \frac{F}{V}(T_f - T) + \left(\frac{-\Delta H}{\rho C_p}\right) K_o \exp\left(\frac{-\Delta E}{RT}\right) C_A - \left(\frac{U_o A}{\rho V C_p}\right)(T - T_j) \qquad (2)$$

where, C_A and C_{Af} : concentration of reactant A in the reactor and feed stream, respectively; R: gas constant; t: time; C_p: heat capacity; F: flow rate (volume); K_o: pre-exponential factor; T: temperature in the reactor; T_f: temperature of feed; T_j: temperature of jacket; U_o: overall heat transfer coefficient; A: area; V: reactor volume; ΔE: activation energy; $(-\Delta H)$: heat of reaction; ρ: density. The design of a Neuro-estimator is discussed in the next section.

Neuro-estimator

A feed-forward artificial neural network (ANN) model is used in this study for the prediction of the states in the CSTR. The ANN structure for the developed estimator is shown in Fig. 2.

The estimator uses Levenberg-Marquardt back propagation training method which is more robust than the standard Gauss-Newton algorithm[9]. The Neuro-estimator has been developed and tested for disturbances in several process variables such as: T_j, T_i and F/V, where temperature (T) is the only input that is used to estimate the concentration (C_A). The input and output parameters for the developed Neuro-estimator are the reactor temperature (T) and product concentration (C_A), respectively. The network training parameters are listed in Table 3.

The developed neuro-estimator, i.e. a feed-forward artificial neural network (F-ANN), has a single hidden layer. The hidden neurons employed a logarithmic sigmoid activation function, whilst the output layer neurons used a linear activation function. The data for the F-ANN is generated from the simulated model developed in MATLAB™– a total of 1382

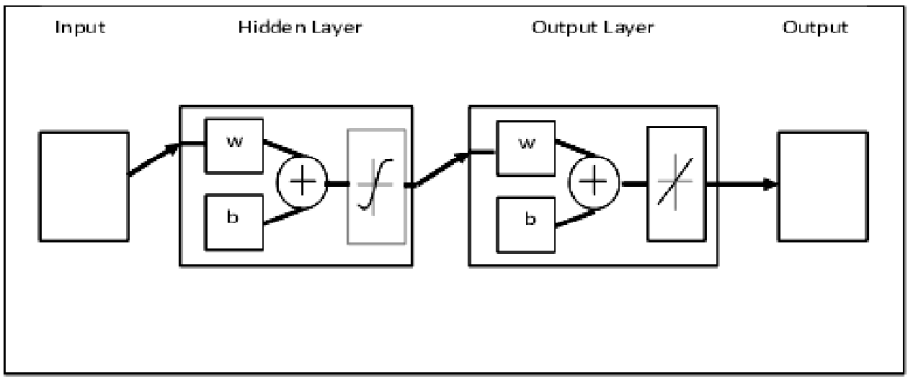

Fig. 2. Schematic diagram of ANN scheme.

Table 3. FANN network training parameters for CSTR

Fix parameters	
Learning rate	0.05
Epochs	1000
Target error goal	10^{-5}
Minimum performance gradient	10^{-5}
Varying parameters	
Number of hidden neuron	1 to 20
Transfer function (hidden layer)	Log-sigmoid (*logsig*)
Transfer function (output layer)	Linear (*purelin*)
Training algorithm	Levenberg-Marquardt back propagation (*trainlm*)

data points were split (using the dividein command) into 70%, 15% and 15% for training, validation and testing.

In F-ANN, the number of hidden neurons is determined using the cross-validation technique. The sum of squared error (SSE) and coefficient of determination (r^2) value is estimated for the training as well as testing data at each node. The network with the least SSE value for both the aforementioned sets is considered suitable for prediction. The regression curve for training, validation and testing is given in Fig. 3. From this analysis, the best topology of the F-ANN is 1-10-1 i.e. one input-10 hidden layer-one output. As noted earlier, the input and output for the developed model is the reactor temperature and concentration, respectively.

In this study, the FANN is developed considering the discrete time of the process. The prediction output is predicted based on the process input $u(t)$ as:

$$\hat{y}(t) = f[u(t)] \tag{3}$$

where $u(t)$, i.e. the input for this case study, is the reactor temperature and $\hat{y}(t)$ is the output (predicted) product concentration.

Controller synthesis

In this study, the controllers are designed to maintain the reactor temperature (T) at the desired set-points. However,

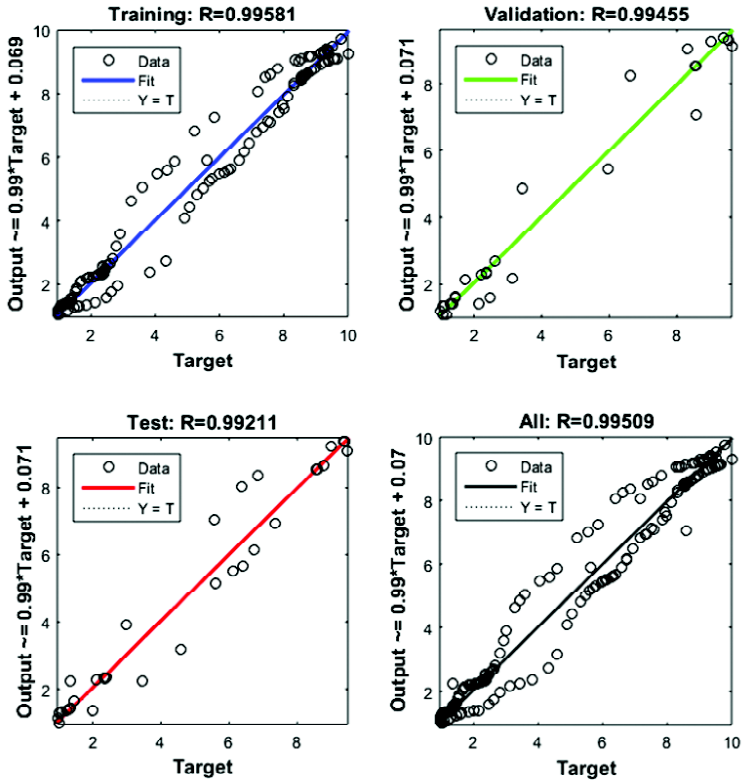

Fig. 3. Regression plots for training, validation and testing.

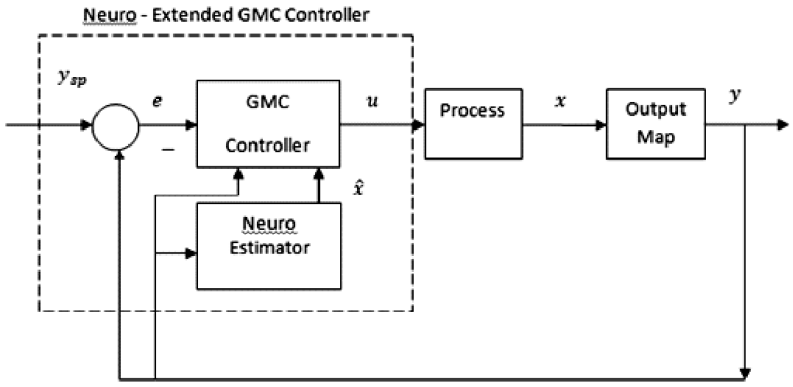

Fig. 4. Neuro-generic model control structure.

the coolant jacket temperature (T_j) is used in this study as a manipulated variable for simplicity in GMC law.

Neuro-GMC controller synthesis

The newly developed Neuro-GMC structure is shown in Fig. 4. It is crucial to provide the information of the states to the GMC control law, which is then clubbed with the developed Neuro-estimator.

The estimator ascertains partially known parameters during a process/predictor mismatch, whereas GMC takes care of the intrinsic non-linearities in the process[10]. The state-space model is given by eqs. (4) and (5).

$$\dot{x} = f(x, d)\theta + g_1(u, x, d) \tag{4}$$

$$y = cx \tag{5}$$

where the state $x \in R^n$, the model parameter $\theta \in R^n$, the measurable disturbance $\in R^n$, the input $u \in R^n$. f and g_1 are matrices of non-linear functions, and c is an unity matrix. The control law can be derived using eq. (6)[11].

$$f(x, d)\theta + g_1(u, x, d) - K_1 e - K_2 \int e\, dt = 0 \tag{6}$$

where e is the error which is equal to $y_{sp} - y$, y_{sp} is the set point, K_1 and K_2 are $n \times n$ tuning parameter matrices. The GMC law comprises of a tuning part which includes the proportional and integral terms. The tuning parameters given in eqs. (7) and (8) can be determined using the relations proposed by Signal and Lee[12].

$$K_{1\,(i,\,i)} = \frac{2\,\tau_{1i}}{\tau_{2i}} \tag{7}$$

$$K_{2\,(i,\,i)} = \frac{1}{\tau_{2i}^2} \tag{8}$$

where τ_{1i} and τ_{2i} are the response times which give the swiftness to the closed loop response. The values of k_1 and k_2 are found to be 3.81 and 0.5, respectively. One can use the aforementioned equations to arrive at the GMC relation described in eqs. (9) and (10).

$$f(x, d)\theta + g_1(u, x, d) = \dot{T} = \frac{F}{V}(T_f - T)$$

$$+ \left(\frac{-\Delta H}{\rho C_p}\right) K_o \exp\left(\frac{-\Delta E}{RT}\right) C_A$$

$$- \left(\frac{U_o A}{\rho V C_p}\right)(T - T_j) - K_1 e - K_2 \int e\, dt \tag{9}$$

Combining the above equation in the GMC state equation, we get:

$$T_j = T - \frac{\rho V C_p}{U_0 A}\left(\frac{F}{V}(T_f - T)\right)$$

$$+ \left(\frac{-\Delta H}{\rho C_p}\right) K_o \in - K_1 e - K_2 \int e\, dt \tag{10}$$

T_j is chosen as the manipulated variable over flow rate, as mentioned above. The control objective covers two cases

which includes controlling the reactor temperature at SS1, SS2 and SS3 (servo mechanism), and secondly to control the reactor temperature when a series of disturbances are imparted in T_j (regulatory mechanism).

IMC controller synthesis

IMC offers good robustness characteristics against external disturbances and model variations.The motivation behind IMC is to club the advantages of different model predictive schemes and avoid prediction errors in cases of severe parametric fluctuations. The IMC design procedure constitutes of two parts: first designing a controller that is optimal with respect to the integral absolute error or integral squared error for a servo study, and secondly a compensator which stabilises the plant[13].

System identification toolbox in MATLAB is used to obtain the transfer function model for this process. Best match for this process is obtained using a second order transfer function with a time delay as follows:

$$G(s) = \frac{0.01065}{s^2 + 0.2527s + 0.009147} \times e^{5s} \quad (11)$$

For the extended IMC, the output y is given by:

$$y = GK_1 r + (1 - GK_1)\frac{P}{1 + PK_2} d_1 + (1 - GK_1)\frac{1}{1 + PK_2} d_2 \quad (12)$$

K_0 is chosen as a PD controller with the form:

$$K_0 = k_0 (\tau_2 s + 1) \quad (13)$$

K_1 is characterized as:

$$K_1 = \frac{(\tau_1 s + 1)\times(\tau_2 s + 1)}{k\times(\gamma s + 1)} \quad (14)$$

where γ is a tuning parameter.

K_2 is chosen as:

$$K_2 = K_c(T_c s + 1) \quad (15)$$

where

$$K_c = \frac{1}{k}\left(\frac{0.533}{\frac{\theta}{\tau}} + 0.746\right) \text{ if } \frac{\theta}{\tau} \le 0.7 \quad (16)$$

$$K_c = \frac{1}{k}\left(\frac{0.490}{\frac{\theta}{\tau}} + 0.694\right) \text{ if } 0.7 \le \frac{\theta}{\tau} \le 1.5 \quad (17)$$

Results and discussion

Neuro-estimator study

This section discusses the performance of the designed estimator and subsequent control structures. The convergence capability of the designed Neuro-estimator is evaluated for disturbances in several process variables.

Disturbance in the jacket temperature (T_j):

Fig. 5 shows the Neuro-estimator responses for disturbances imparted in T_j. The initial coolant temperature is 298 K which is increased to 327.8 K at 50 h (Fig. 5c), resulting in the increase in reactor temperature to 384 K (Fig. 5b). A decrease in the effluent temperature to 368.1 K (i.e. SS2) is obtained with a reduction of the coolant temperature to 298 K at 100 h.

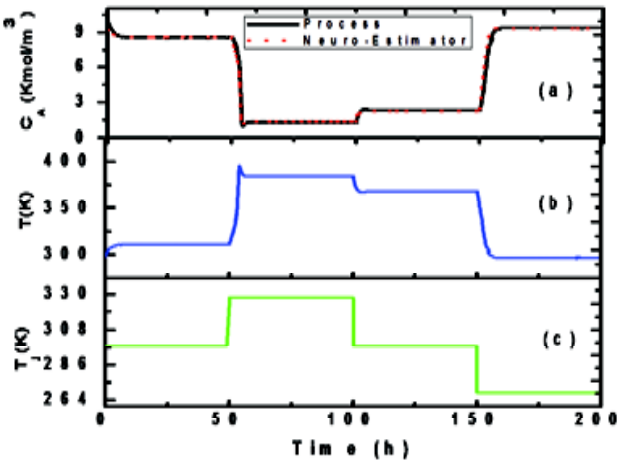

Fig. 5. Neuro-estimator responses for changes in the jacket temperature T_j: (a) reactor concentration, (b) reactor temperature and (c) jacket temperature.

However, the reactor temperature does not reach the initial steady state. This clearly demonstrates the multiplicity present in the CSTR. A further 10% decrease in the coolant temperature (T_j) at 150 h causes the outlet temperature (T) to decrease even further. A good match has been obtained between the developed Neuro-estimator and process model (considered to be a true process) for the concentration profile. This shows a good convergence capability of the developed Neuro-estimator.

Disturbance in the inlet temperature (T_i):

Fig. 6 depicts the Neuro-estimator responses for a series of step changes in T_i. A periodic fluctuation is imparted in the inlet temperature; the inlet temperature is at an initial value of 298 K during 0–50 h. The temperature is further increased to 327.8 K i.e. 10% increment from the initial value for the next 50 h until 100 h. This results in increased effluent temperature to a 407 K.

Further, the inlet temperature is brought back to its initial value of 298 K, but the effluent temperature fails to reach the first steady state SS1 (depicting the multiplicity involved in the system) and settles instead at 368.1 K i.e. SS2. The inlet stream temperature is maintained at 268.2 K from 150 h to 200 h obtaining a sudden decrease in the effluent temperature. The system exhibits nonlinearity which can be observed through the reactor effluent temperature plot (Fig. 6b). High level of convergence is achieved through the designed Neuro-estimator.

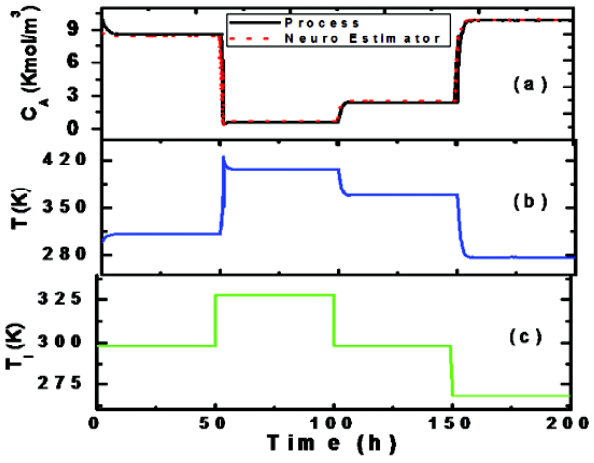

Fig. 6. Neuro-estimator responses for changes in the inlet temperature T_i: (a) reactor concentration, (b) reactor temperature and (c) inlet temperature.

Controller performance evaluation

Servo-study:

Fig. 7 shows the controller performance for a series of step changes in the controlled variable i.e. reactor temperature (T) (shown in black). The reactor temperature undergoes a step-wise increment until 100 h followed by decrease until 250 h. In essence, the temperature is shifted from SS1 (311.2 K) to SS2 (339.1 K) at 50 h and then to SS3 (368.1 K) at 100 h. Later, it is brought back to SS1 at 200 h. Although, Neuro-GMC shows a slightly sluggish response, it is able to track the set-points in minimum settling time and moderate rise-time and TV (see Table 4). The extended-IMC controller shows a delayed response with a high TV value of 551 and a moderate settling time of 21 h.

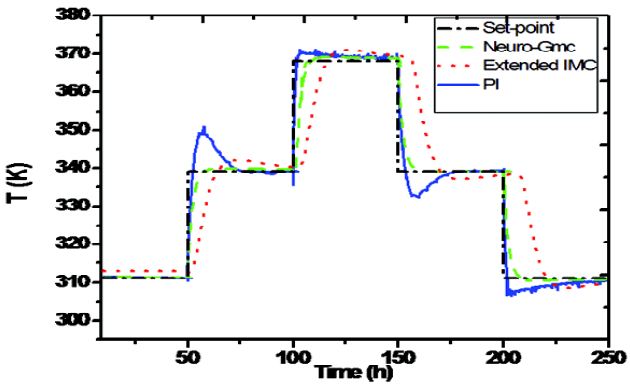

Fig. 7. Servo-study: Reactor temperature.

Note that the steady-state and bias output are different for extended IMC (see Fig. 7) when compared with the other two controllers, which is due to a process-model mismatch. On the contrary, Neuro-GMC, despite being a model based controller as IMC, shows superior performance due to an efficient Neuro-estimator which works collectively with the GMC law to ascertain accurate user-defined set points. It is noticed that the Neuro-GMC requires minimum effort to attain the steady states as opposed to the other two controllers for the servo-study (see Table 4). PI shows an overshoot and delayed settling time as compared to Neuro-GMC.

Regulatory study:

A regulatory study has been performed for the system where a series of fluctuations in the *F/V* is imparted. The system is made to operate at SS2 (unstable and challenging node) by providing the set-point as 339.1 K. For regulatory control, the performance of the controller is evaluated based on TV which is an indicator of the control effort required for the control system to attain the steady state after a disturbance. An increase in the *F/V* ratio until 100 h results in reduced temperatures. The *F/V* is subsequently brought back to 1.0 at 100 h and maintained at a constant value until 150 h. The ratio is further decreased to 0.9 till 200 h and brought back to unity at 200 h (see Fig. 8). This reduction in ratio manifests in an increasing temperature profile. Again, the Neuro-GMC outperforms PI and the extended IMC due to its faster response and effective set-point tracking. PI shows an overshoot whereas extended IMC takes more time to stabilize the reactor temperature for fluctuations in the flow rate. Neuro-GMC depicts a robust and a swift response (Fig. 8). Although, it can be seen that the extended IMC has the lowest TV value describing the least control effort required against fluctuations in the flow rate, it is not as accurate as other two controllers. This can be inferred from different steady states and bias output values for extended IMC (see Fig. 8) controller. PI has the highest TV value suggesting the highest control effort amongst Neuro-GMC and the extended IMC. From Table 4, it is clear that Neuro-GMC displays superior performance than the other two controllers in terms of TV, settling time and the rise time. For the servo-study, the proposed Neuro-GMC scheme is better in terms of all the tested criteria, viz. TV, settling time and rise time. On the other hand, IMC scheme shows the smallest TV for the regulatory case. Although less TV is attractive, the performance of IMC is not acceptable in this case because of a poor set point tracking as a consequence of model-process mismatch, as observed from Fig. 8.

Table 4. Controller performance evaluation

Control scheme	Servo			Regulatory
	TV	Settling time (h)	Rise time (h)	TV
Neuro-GMC	380	12	8	486
IMC	551	21	18	349
PI	703	46	3	795

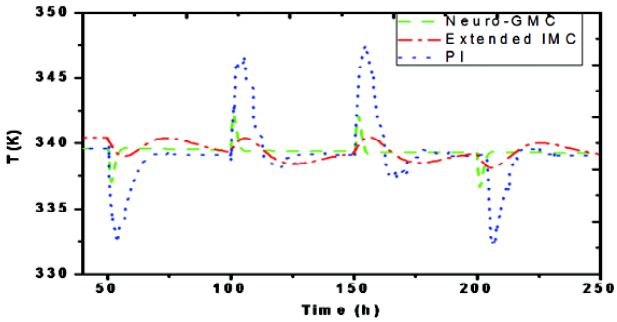

Fig. 8. Regulatory study: Reactor temperature.

Conclusions

This work developed a high quality control scheme that could cope multiplicity and non-linearity issues of a CSTR. First, a Neuro-estimator, developed using feed forward neural network has provided fine open loop tracking performance. Then it was clubbed with a model based GMC controller to develop a hybrid 'Neuro-GMC' control scheme. The Neuro-GMC has multiple benefits, such as simple design, easy tuning and better performance. Later, a closed loop performance of the three controllers, namely Neuro-GMC, extended IMC and conventional PI, has been evaluated. Hybrid Neuro-GMC control scheme has been found to yield superior performance than the extended IMC and conventional PI controller in terms of TV, settling time and rise time. Extended IMC, another advanced model based controller, showed a slightly poorer performance due to inaccurate model identification, whereas Neuro-GMC showed excellent results due to the efficient neural estimator. The settling time and TV for Neuro-GMC are lesser than those of extended IMC and conventional PI that accentuates that Neuro-GMC requires lesser control efforts to stabilize the process.

References

1. R. Su, *Sys. Control Lett.,* 1982, **2**, 48.
2. L. Hunt, S. Renjeng and G. Meyer, *IEEE T. Automat. Contr.,* 1983, **28**, 24.
3. I. M. Mujtaba, N. Aziz and M. A. Hussain, *Chem. Eng. Res. Des.,* 2006, **84**, 635.
4. J. Czeczot, *Chem. Eng. Process,* 2006, **45**, 359.
5. D. K. Rollins and Y. Mei, *Chemical Engineering Research and Design*, 2018, **136**, 806.

6. A. K. Jana, *Int. J. Chem. React. Eng.*, 2007, **5**, 1.
7. B. Guo, A. Jiang, X. Hua and A. Jutan, *Chem. Eng. Sci.,* 2001, **56**, 6781.
8. V. Srivastava and S. Srivastava, *Journal of Information and Optimization Sciences*, 2019, **40(2)**, 329.
9. H. Yu and B. M. Wilamowski, "Levenberg–marquardt Training in Industrial Electronics Handbook", 2nd ed., CRC Press, 2011, **12**, 12-1-12-5.
10. J. K. J. Prakash, D. S. Patle and A. K. Jana, *ISA T*, 2011, **51**, 357.
11. P. L. Lee and G. R. Sullivan, *Comp. Chem. Eng.*, 1988, **12**, 573.
12. P. D. Signal and P. L. Lee, *Chem. Eng. Comm.*, 1992, **115**, 35.
13. W. Tan, H. J. Marquez and, T. Chen, *J. Process Contr.,* 2003, **13**, 203.